

Chapter 33

Liquid-Flow Measurements in Silicon Dioxide Channels with Micron-Sized Dimension

G. Barillaro, A. Diligenti and L. M. Strambini

Abstract Flow measurements on silicon dioxide microchannels featuring inner cross-section as low as $16 \mu\text{m}^2$ and aspect-ratio as high as 50 have been performed using liquids with different dynamic viscosities. The microchannels, arranged in a square array with density of 1×10^6 channel/ cm^2 , are embedded into a silicon substrate and connected to a reservoir grooved on the backside of the substrate. Flow measurements were performed by using an original, purposely designed system. In this work, details on both the measurement systems and the flow properties of such a small channels are reported and discussed.

33.1 Introduction

In last two decades, driven by the development of microfluidic systems for biomedical and optofluidic applications, significant attention has been paid to liquid-flow in microchannels. Although the liquid-flow properties of tubes with inner side (diameter) of tens of microns have been extensively studied [1–4] and reported to obey the Hagen–Poiseuille (H–P) law, only a few studies on circular tubes with inner diameter of a few microns have been reported so far. On the other hand, due to the trend of scaling-down both microfluidic devices and systems, understanding fluid-flow in micron-sized tubes is becoming more and more important.

In this paper flow measurements on silicon dioxide microchannels with length of $200 \mu\text{m}$ and inner side of $4 \mu\text{m}$ (square section) are reported, along with a brief

G. Barillaro (✉) · A. Diligenti · L. M. Strambini
Dipartimento di Ingegneria dell'Informazione: Elettronica, Informatica,
Telecomunicazioni, Università di Pisa, via G. Caruso 16, 56122, Pisa, Italy
e-mail: g.barillaro@iet.unipi.it

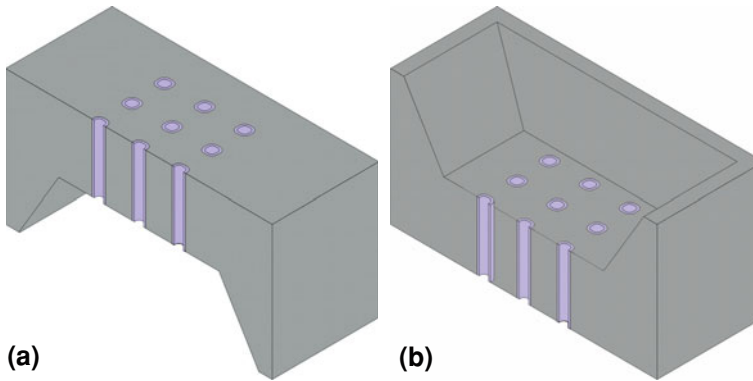


Fig. 33.1 Sketch of the silicon chip used for fluid-flow measurements, consisting of an array of microchannels embedded into a silicon substrate in communication with a reservoir etched on the backside of the chip: **a** *top-view* of the chip; **b** *bottom-view* of the chip

description of the fabrication process. Moreover, the experimental system purposely set up to perform flow measurements is also described.

33.2 Fabrication Process

Figure 33.1 shows a sketch of the silicon chip used for microchannel liquid-flow characterization. The chip consists of an array of high-aspect ratio (up to 50) hollow silicon dioxide channels, with inner side of $4\ \mu\text{m}$, length of $200\ \mu\text{m}$, density of 10^6 needles/ cm^2 , embedded into a silicon substrate and in communication with a reservoir grooved on the backside of the chip.

The fabrication process consists of the following main steps: (1) photo-electrochemical etching (PEC) of a *n*-type silicon substrate ((100) oriented, with resistivity of $3\text{--}8\ \Omega\ \text{cm}$ and thickness of $550\ \mu\text{m}$) allowing a deep, ordered macropore array to be etched [5–8]; (2) wet thermal oxidation of the macropores to obtain silicon dioxide micropipes, still closed at their bottom-side; (3) anisotropic silicon wet etching (TMAH) on the backside of the substrate to define a reservoir, and (4) silicon dioxide wet etching (BHF) on the backside of the substrate to open the micropipes bottom-side and obtain hollow microchannels in communication with the reservoir.

Vertical and horizontal uniformity of the channels basically depends on two technological steps: (1) the electrochemical etching step and (2) the thermal oxidation step. If good uniformity was expected for the PEC step, due to the feedback mechanism ruling macropore growth [5–8], the same result was not easily predictable for thermal oxidation of deep macropores. Measurements of the oxide thickness along the pore axis, performed by SEM observation of the cross-section of oxidized samples, confirmed that no appreciable changes in the oxide thickness occur along the macropore axis, at least for depths up to $200\ \mu\text{m}$.

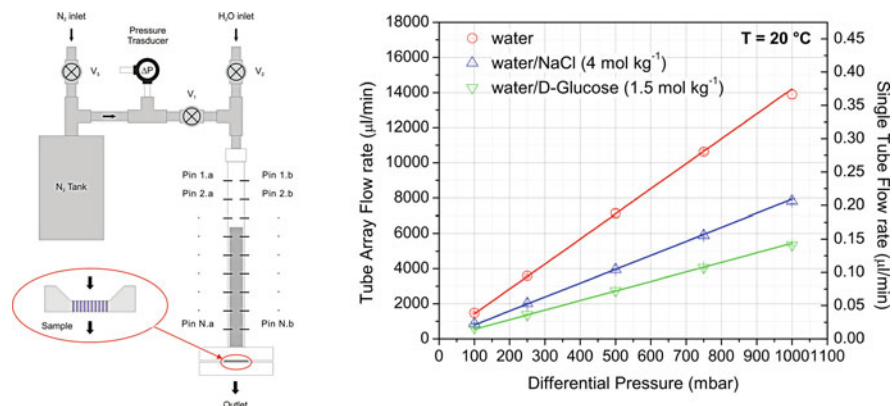


Fig. 33.2 (left) Experimental setup used for liquid-flow measurements. (right) Flow rate versus pressure drop for an array of 38,000 silicon-dioxide tubes with square section for three different solutions

33.3 Experimental Set-Up and Flow Measurements

The experimental setup used for liquid-flow measurements is sketched in Fig. 33.2. The silicon chip (inset in Fig. 33.2 left), containing the microchannel array with geometrical characteristics as here above described, was put at the end of a graduated pipe, which was filled with the liquid under investigation. A number of couples of electrodes placed at regular distance (2 cm) along the pipe were used to monitor the liquid level by resistance value measurements. A constant differential pressure drop $P_D = P_{in} - P_{out}$ (P_{out} being the reference atmospheric pressure) was maintained between the top of the liquid column and the chip outlet during the whole experiment, thanks to a reservoir with a volume ($4,300 \text{ cm}^3$) much larger than the pipe (about 10 cm^3). A maximum relative pressure variation $\Delta P_D/P_D$ of about 2×10^{-3} was measured during experiments.

Liquid-flow measurements as a function of the pressure drop were performed with deionized water (DI H_2O) and, NaCl (4 mol kg^{-1}), D-glucose (1.5 mol kg^{-1}) aqueous solutions, which have dynamic viscosities of 1.0, 1.5, 2.24 mPa s, respectively [9]. The viscosity of the three test solutions was measured by means of a standard viscosimeter and resulted in good agreement with literature values [9]. Liquid-flow measurements were carried out using differential pressures P_D in the range 100–1,000 mbar.

In order to avoid partial or full obstruction of the channel array during measurements, the solutions were filtered with $0.22 \text{ }\mu\text{m}$ filters before their introduction in the graduated pipe. Moreover, in order to verify possible channel obstruction, before and after each measurement cycle (with a given liquid in the whole P_D range) a control measurement was performed at $P_D = 500 \text{ mbar}$ using DI H_2O . Control measurements confirmed that the same number of channels in the array was actually active during flow measurements with the three tested solutions.

Experimental results on the three tested solutions are resumed in Fig. 33.2, which shows the liquid-flow rate F versus the differential pressure P_D , both for the whole microchannel array (left scale) and the single tube (right scale). Measurement results highlight a linear relationship between F and P_D for each microtube, according to the Hagen–Poiseuille law:

$$F = \frac{A}{L} \frac{2D_h^2}{C_{fr}\mu} P_D \quad (33.1)$$

where A is the cross-section area, L is the channel length, D_h is the hydraulic diameter, $C_{fr} = 57$ is the friction coefficient for square section, and μ is the dynamic viscosity, even if the channel section is only a few (less than 16) μm^2 . The number of active channels is about 38,000, as obtained both by SEM observations and by best-fitting of experimental data using the Hagen–Poiseuille law.

33.4 Conclusions

In this work the liquid-flow properties of high aspect-ratio microchannels have been experimentally investigated using three test solutions with different dynamic viscosities. Flow measurements, to our knowledge performed for the first time on channels with cross-section of a few square microns, highlighted that: (i) the Hagen–Poiseuille law still holds for tubes with such a reduced cross-section area; (ii) an array of 38,000 channels with cross-section of about 16 μm^2 allows solutions of sanitary interest to be delivered at rate comparable with that of commonly used macroscopic hypodermic needles. The latter result is very important for drug delivery application, as the microchannel fabrication process reported in this work can be easily modified for the formation of an array of pain-free microneedles to be inserted in the outermost layer of the skin for transdermal drug delivery.

Acknowledgments This work was supported by Fondazione Cassa di Risparmio di Pisa, Pisa, Italy in the frame of the Project “Microsistema integrato per l’iniezione sottocutanea controllata di piccole quantità di medicinali” (“Integrated microsystem for the controlled delivery of small drug quantities”).

References

1. Jiang XN, Zhou ZY, Huang XY, Liu CY (1997) Laminar flow through microchannels used for microscale cooling systems. In: Proceedings of the electronic packaging technology conference, EPTC, pp 119–122
2. Mala GhM, Li D (1999) Flow characteristics of water in microtubes. *Int J Heat Fluid Flow* 20:142–148
3. Park H, Pak JJ, Son SY, Lim G, Song I (2003) Fabrication of a microchannel integrated with inner sensors and the analysis of its laminar flow characteristics. *Sens Actuators A* 103: 317–329

4. Steinke ME, Kandlikar SG (2006) Single-phase liquid friction factors in microchannels. *Int J Thermal Sci* 45:1073–1083
5. Lehmann V (1993) The physics of macropore formation in low doped n-type silicon. *J Electrochem Soc* 140:2836–2843
6. Lehmann V, Gruning U (1997) The limits of macropore array fabrication. *Thin Solid Films* 297:13–17
7. Barillaro G, Nannini A, Piotto M (2002) Electrochemical etching in HF solution for silicon micromachining. *Sens Actuators A* 102:195–201
8. Barillaro G, Bruschi P, Diligenti A, Nannini A (2005) Fabrication of regular silicon microstructures by photo-electrochemical etching of silicon. *Phys Stat Sol (c)* 2:3198–3202
9. Comesaa JF, Otero JJ, Garcia E, Correa A (2003) Densities and viscosities of ternary systems of water + glucose + sodium chloride at several temperatures. *J Chem Eng Data* 48:362–366